Wang, F. et al. Fourier transform ion cyclotron resonance mass spectrometric detection of small Ca(2+)-induced conformational changes in the regulatory domain of human cardiac trop...

ARTICLE *in* JOURNAL OF THE AMERICAN SOCIETY FOR MASS SPECTROMETRY · SEPTEMBER 1999

Impact Factor: 2.95 · DOI: 10.1016/S1044-0305(99)00039-2 · Source: PubMed

Fourier Transform Ion Cyclotron Resonance Mass Spectrometric Detection of Small Ca^{2+}-Induced Conformational Changes in the Regulatory Domain of Human Cardiac Troponin C

Fang Wang, Weiqun Li,* Mark R. Emmett, and Alan G. Marshall*
Center for Interdisciplinary Magnetic Resonance, National High Magnetic Field Laboratory, Florida State University, Tallahassee, Florida, USA

David Corson and Brian D. Sykes
Department of Biochemistry, University of Alberta, Edmonton, Alberta, Canada

Troponin C (TnC), a calcium-binding protein of the thin filament of muscle, plays a regulatory role in skeletal and cardiac muscle contraction. NMR reveals a small conformational change in the cardiac regulatory N-terminal domain of TnC (cNTnC) on binding of Ca^{2+} such that the total exposed hydrophobic surface area increases very slightly from 3090 ± 86 Å^2 for apo-cNTnC to 3108 ± 71 Å^2 for Ca^{2+}-cNTnC. Here, we show that measurement of solvent accessibility for backbone amide protons by means of solution-phase hydrogen/deuterium (H/D) exchange followed by pepsin digestion, high-performance liquid chromatography, and electrospray ionization high-field (9.4 T) Fourier transform Ion cyclotron resonance mass spectrometry is sufficiently sensitive to detect such small ligand binding-induced conformational changes of that protein. The extent of deuterium incorporation increases significantly on binding of Ca^{2+} for each of four proteolytic segments derived from pepsin digestion of the apo- and Ca^{2+}-saturated forms of cNTnC. The present results demonstrate that H/D exchange monitored by mass spectrometry can be sufficiently sensitive to detect and identify even very small conformational changes in proteins, and should therefore be especially informative for proteins too large (or too insoluble or otherwise intractable) for NMR analysis. (J Am Soc Mass Spectrom 1999, 10, 703–710) © 1999 American Society for Mass Spectrometry

For about three decades, protein amide hydrogen isotopic exchange rates have provided information about the higher-order structure, structural changes, and structural dynamics of proteins [1–5]. With the advent of electrospray ionization mass spectrometry (ESI-MS), hydrogen/deuterium exchange for a protein as a whole could be monitored quickly and easily by mass spectrometry (MS), to characterize protein denaturation [6], folding intermediates [7], conformational states [8–10], and structural perturbations induced by binding of ligands or other proteins [11].

H/D exchange followed by proteolytic digestion and on-line liquid chromatography/mass spectrometry (LC/MS) serves to localize the solvent accessibility within individual peptide segments of a protein [12–14]. That approach makes it possible to define the effect of mutations on protein stability [15–18], and to characterize higher-order structure and dynamics of proteins [19–21] as well as protein conformational changes induced by ligand binding [9, 18, 22]. In particular, Fourier transform ion cyclotron resonance mass spectrometry (FT-ICR MS) offers several advantages for H/D exchange analysis because of its ultrahigh mass resolving power [23–32]. Finally, the upper mass limit for FT-ICR MS (and the precision with which the number of incorporated deuteriums may be measured) may be extended by almost an order of magnitude by expression of the protein from media doubly depleted in ^{13}C and ^{15}N [33].

Troponin C (TnC) is a calcium-binding protein of the thin filament of muscle and plays a regulatory role in skeletal and cardiac muscle contraction. The conformational changes of TnC induced by Ca^{2+} binding are

Address reprint requests to Dr. Alan G. Marshall, Center for Interdisciplinary Magnetic Resonance, National High Magnetic Field Laboratory, 1800 East Paul Dirac Drive, Florida State University, Tallahassee, FL 32310. E-mail: marshall@magnet.fsu.edu

* Member of Department of Chemistry, Florida State University.

1044-0305/99/$20.00
PII S1044-0305(99)00039-2

Received January 6, 1999
Revised March 30, 1999
Accepted March 31, 1999

believed to be transmitted via the linkage between TnC and TnI (troponin I) within the three-subunit troponin complex, so as to initiate a cascade of structural changes in the thin filament complex leading to muscle contraction [34]. The two isoforms of the TnC are found in fast skeletal muscle TnC (sTnC) and slow skeletal and cardiac muscle TnC (cTnC). The X-ray structure of avian sTnC shows a highly α-helical protein with two domains: C-terminal and N-terminal [35]. Each domain contains two Ca^{2+}-coordinating E-F hands: i.e., two perpendicular α-helices and a 12 amino residue loop between them. The two Ca^{2+} binding sites (I and II) in the N terminus of TnC are *regulatory* sites [36–39] and have a lower affinity for Ca^{2+} relative to the *structural* binding sites (III and IV) [40] in the C terminus of TnC.

The measured Ca^{2+} binding constant for (regulatory) site II in the N domain is the same as that measured for intact cardiac TnC [41]; similarly, Ca^{2+} binding to the N domain of skeletal TnC remains unchanged when it is separated from intact skeletal TnC [42, 43]. Thus, NMR analysis has concentrated on the smaller N domain rather than on the full troponin C protein.

The solution NMR structure of the N-terminal domain of *skeletal* TnC (sNTnC) reveals an "opening" of the structure and the concomitant exposure of a substantial hydrophobic surface area upon Ca^{2+} binding to sNTnC [44]. The primary structure of cNTnC is highly similar to that of sNTnC. However, site-specific mutation of critical side chains (D29L and D31A) and an insertion (Val-28) in cNTnC abolish the ability of one of the regulatory Ca^{2+}-binding sites to coordinate Ca^{2+}. In contrast, NMR fails to show any opening of the domain and the concomitant exposure of a substantial hydrophobic surface area for *cardiac* N-domain TnC (cNTnC) upon binding of Ca^{2+} [41, 45, 46]. cNTnC remains essentially in the "closed" conformation in its Ca^{2+}-saturated state, with only a minor conformational change compared to apo-cNTnC.

Therefore, in this paper, we undertake to measure backbone amide hydrogen/deuterium exchange for human apo- and Ca^{2+}-saturated forms of the N domain isolated from human cardiac TnC by use of LC-ESI FT-ICR MS, to see if mass spectrometry can detect small Ca^{2+}-induced conformational changes barely detectable by NMR.

Experimental

Protein Preparation

Plasmid for the expression of the N domain of cardiac troponin C was provided by Dr. Murali Chandra in the laboratory of Professor R. John Solaro in the Department of Physiology and Biophysics, College of Medicine, University of Illinois, Chicago. *E. coli* cells, strain BL21(DE3)pLysS, were transformed according to standard methodologies [45]. Several colonies from the plates of the transformed cells were used to inoculate TY media (NaCl 2.5 gm/L Bacto-trytone 8.0 gm/L; yeast extract 5.0 gm/L) which were grown to O.D. 1.0. 5 mL of these cells were used to inoculate 500 mL of limited media (NaH_2PO_4—12 gm/L; K_2HPO_4—6 gm/L; NH_4SO_4—1.1 gm/L; glucose—3 gm/L). All cultures were grown with the addition of 1 mL/L of 5% ampicillin solution and 1 mL/L of 2.5% chloramphenicol solution. 99.9% ^{15}N depleted ammonium sulfate and 99.9% ^{13}C depleted glucose, both obtained from Isotech (Miamisberg, OH), constituted the sole nitrogen and carbon sources, respectively. Cells were grown under these conditions to O.D. 0.71, induced with IPTG, and allowed to incubate for 3 h. The cells were then centrifuged and resuspended in 50 mM tris HCl buffer at pH 8.0, French-pressed, and the lysate applied to a 100 ml DEAE A-25 Sepharose® column. The purified protein was eluted with 1 L of a 0.10 $\rightarrow$ 0.55 M NaCl gradient in 50 mM Tris HCl, 2 mM $MgCl_2$ buffer, and then dialyzed for 3 days versus deionized H_2O with mercaptoethanol present, and lyophilized [41].

Materials

Pepsin was obtained from Worthington, Co. (Lakewood, NJ), and D_2O (99.9 atom % D) from Aldrich Chemical Co. (Milwaukee, WI). All other chemicals and reagents were of the highest grade commercially available.

Hydrogen Exchange

H/D exchange was initiated by 20-fold dilution, namely, by adding 20 μL of a 1 mM ^{13}C, ^{15}N-depleted cNTnC solution in 10 mM imidazole buffer, pH 6.7, 100 mM KCl, 15 mM DTT, and 10 mM EDTA (for Ca^{2+}-free TnC) or 10 mM $CaCl_2$ (for Ca^{2+}-saturated cNTnC), to 380 μL of 99.9 atom% D_2O buffer containing 10 mM imidazole and 100 mM KCl, $pH_{reading}$ 6.3. Solutions were maintained at 25 °C in a water bath, and incubated for each of several H/D exchange periods. At appropriate intervals, aliquots of the cNTnC solution were quenched by the addition of an equal volume of 0.5 M phosphate buffer, pH 2.2 in H_2O, and immediately frozen in liquid N_2. The samples were stored at −70 °C until analysis.

Pepsin Digestion

The deuterated protein was thawed on ice. A 90-μL aliquot of deuterated protein solution was added to 14 μL of 80 μM pepsin in 0.5 M phosphate buffer, pH 2.2, injected onto a 10-μL injection loop, and allowed to digest for 3 min at 0 °C in the loop prior to HPLC analysis.

LC-ESI FT-ICR MS Analysis of the Digested Peptides of Deuterated cNTnC

Extent of deuterium incorporation into cNTnC and localization was determined by LC-ESI FT-ICR MS

analysis. Acetonitrile gradients at 30 μL/min were generated with a Shimadzu HPLC equipped with two LC-10AD pumps. Solvent A was 94.5% H_2O containing 5% acetonitrile and 0.5% formic acid (pH 2.3), and solvent B was 80% acetonitrile containing 19.5% H_2O and 0.5% formic acid. A low volume static mixing tee was used to minimize the delay period for HPLC. The solvent precooling coil, static mixing tee, Rheodyne injector, and column were immersed in an ice bath (0 °C) to minimize back exchange with HPLC solvents. Aliquots (10 μL) of the exchanged and quenched pepsin digests were loaded onto a Vydac 1.0 × 50 mm C_4 or C_8 column, respectively. After desalting at 5% B for 2 min, the peptic peptides eluted between 4.2 and 6.5 min with a 7-min 5%–50% B gradient. The column effluent (30 μL/min) was delivered directly to the mass spectrometer without flow split.

To account for deuterium gain or loss under quenched conditions, we prepared two control samples [12]. A "zero-deuteration" control was prepared by diluting the protein solution directly into a 1:1 (*v/v*) mixture of deuterated buffer and quench buffer. A "full-deuteration" control was prepared by 1:20 (*v/v*) dilution of cNTnC into 2 M urea-d_4 in D_2O solution and incubation for 1.0 h at 55 °C. The deuterium content, *D*, for each partially deuterated protein (or segment) may be calculated from [13]:

$$D = \frac{m - m_{0\%}}{m_{100\% - m_{0\%}}} \times H \quad (1)$$

in which *H* is the total number of backbone amide hydrogens in the protein (or its segment), e.g., $H = 86$ for cNTnC after taking into account that the N-terminal residue and proline linkages have no exchangeable amide hydrogens. In eq 1, $m_{0\%}$, m, and $m_{100\%}$ are the average (i.e., the centroid of the isotope envelope) molecular weights for the 0% control, partially deuterated, and 100% control protein. All deuterium contents reported in this paper were calculated from eq 1, in which *H* is the total number of backbone amide hydrogens for the segment in question. Back exchange for each proteolytic peptide was determined from the difference between the theoretical mass for maximally (95% D_2O) amide-deuterated species and the experimental mass determined after LC/MS analysis. For the intact protein, the extent of back exchange was ~19% (versus 38%–62% for various proteolytic peptides) during quench and LC/MS analysis. Those values are consistent with the 40%–50% of overall back exchange reported by other authors [16, 20] and more recent 18%–55% values [18, 22].

Identification of Proteolytic Segments

cNTnC was digested with pepsin (~2:1 substrate:enzyme mole ratio) at pH meter reading 2.2 and 0 °C for 3 min, then subjected to HPLC/MS analysis. Mass resolving power, $m/\Delta m_{50\%}$, (in which $\Delta m_{50\%}$ is the mass-domain peak full width at half-maximum peak height) ranged between 50,000 and 120,000, depending on the peptide mass-to-charge ratio (m/z).

Table 1. Illustration of peptic peptide identification based on FT-ICR accurate mass measurement. The experimental peptide monoisotopic mass (i.e., all carbons are ^{12}C, all nitrogens are ^{14}N, all oxygens are ^{18}O, all hydrogens are ^{1}H, and all sulfurs are ^{32}S) is 829.65 ± 0.09 for $(M + 4H)^{4+}$, or $M = (829.65 * 4) - (4 * 1.0073) = 3314.6 \pm 0.4$ Da. [The mass of a proton is 1.0078 (^{1}H atom) − 0.0005 (electron) = 1.0073.] The table lists all of the possible cNTnC fragment monoisotopic masses within 1.5 Da of the experimental value. Only one, [C] I36-V64 [D], falls within 100 ppm, and identifies the correct fragment. The brackets denote the amino acid preceding the amino-terminus (or following the carboxy-terminus) of the segment before proteolysis.

Peptide segment	Monoisotopic mass	Deviation from experimental value (ppm)
[E] E14-G43 [K]	3315.63	313
[Q] K17-R46 [M]	3315.70	333
[C] I36-V64 [D]	3314.65	18

Mass Spectrometry

Mass analyses were performed with a homebuilt FT-ICR mass spectrometer, based on a passively shielded 9.4 tesla 200-mm diameter horizontal-bore superconductive magnet, and equipped with a homebuilt external electrospray interface described elsewhere [25, 47]. An Odyssey™ data system (Finnigan FTMS, Madison, Wisconsin) acquired time-domain ICR data, Fourier transformed it, applied Hanning apodization, and processed the discrete mass spectrum into a peak list. Direct-mode excitation was by frequency sweep from 480,988 Hz (*m/z* 300 for peptides) at a sweep rate of 130 Hz μs^{-1}. Time-domain data size was 128 kword. The

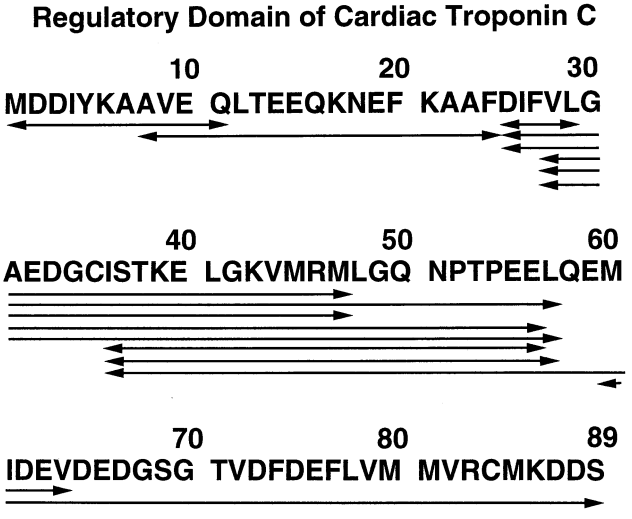

Figure 1. Amino acid sequence of cNTnC, showing the pepsin-cleaved mass-identified fragments (double-ended arrows) for which deuterium incorporation was measured.

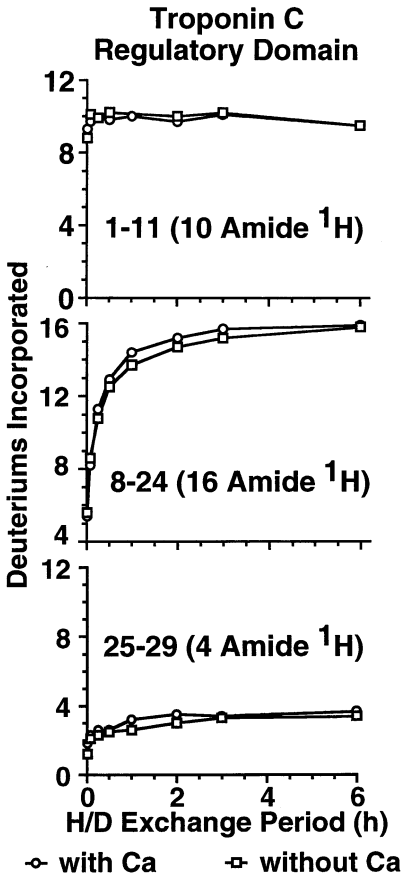

Figure 2. Time course for deuterium uptake for each of three different segments from cNTnC in the presence (open circle) or absence (open square) of Ca^{2+}, each showing no difference in rate of deuterium uptake upon Ca^{2+} binding. The number of potentially exchangeable backbone amide hydrogens in each segment is shown in each panel.

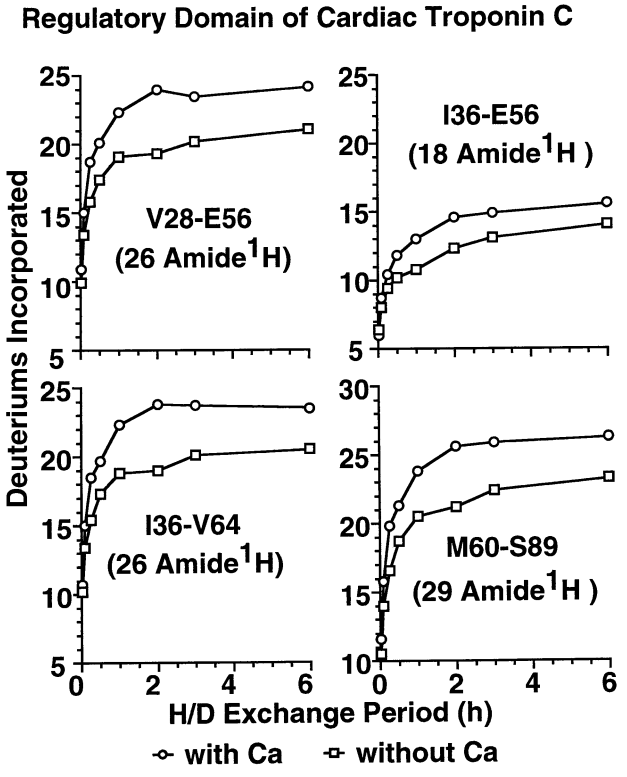

Figure 3. Time course for deuterium uptake for each of four other segments from cNTnC in the presence (open circle) or absence (open square) of Ca^{2+}, each showing significant increase in rate of deuterium uptake upon Ca^{2+} binding. The number of potentially exchangeable backbone amide hydrogens in each segment is shown in each panel.

peak list was further analyzed with homewritten software to display the extent of deuterium uptake by pepsin-digest peptides [21].

Results and Discussion

Deuterium Incorporation for Intact cNTnC

TnC is an EF-hand calcium-binding protein of thin filaments, with a single polypeptide chain molecular weight of 18 kDa. It consists of similar N- and C-terminal globular domains (NTnC and CTnC). The cardiac N-terminal domain of troponin C (cNTnC) contains one Ca^{2+}-binding regulatory site (2.6-μM dissociation constant). The NMR structure of cNTnC contains five α-helices (N, A, B, C, D) and two short β-sheets [45]. The B and C helices reorient slightly relative to the NAD unit upon Ca^{2+} binding. For H/D exchange of Ca^{2+}-saturated cNTnC, we used 500 μM of Ca^{2+} and 50 μM cNTnC, so that ~96% of the cNTnC should be in the Ca^{2+}-bound form. Although Ca^{2+} is present at 10-fold excess over protein (to ensure high saturation of strong-site Ca^{2+} binding), prior NMR shows that the resulting nonspecific Ca^{2+} binding does not affect the protein conformation [41].

Mass Spectrometric Identification of Pepsin-Cleavaged Segments of cNTnC

We performed H/D exchange followed by pepsin digestion to cleave the protein somewhat nonspecifically to yield many peptide fragments, each of which could then be identified (and its deuterium uptake determined) by ESI FT-ICR MS. The peptic peptides derived from cNTnC could be assigned from data from a single LC run by ESI FT-ICR MS with external calibration (<30 ppm mass accuracy). Use of ^{13}C, ^{15}N isotopically doubly depleted protein made it possible to assign each of the various peptic peptides solely from its accurate monoisotopic mass (i.e., no need for tandem mass spectrometry). For example (see Table 1), search of the cNTnC amino acid sequence yields three peptides (residues 14–43, 17–46, and 36–64), each of whose monoisotopic molecular mass agrees to within ~1.5 Da with a particular experimental peptide mass of 3314.6 ± 0.4 Da. However, the monoisotopic mass of only one of those peptides (residues 36–64) falls within 100 ppm of the experimental value. Remarkably, *10 of the 12 peptic peptides generated from cNTnC could be*

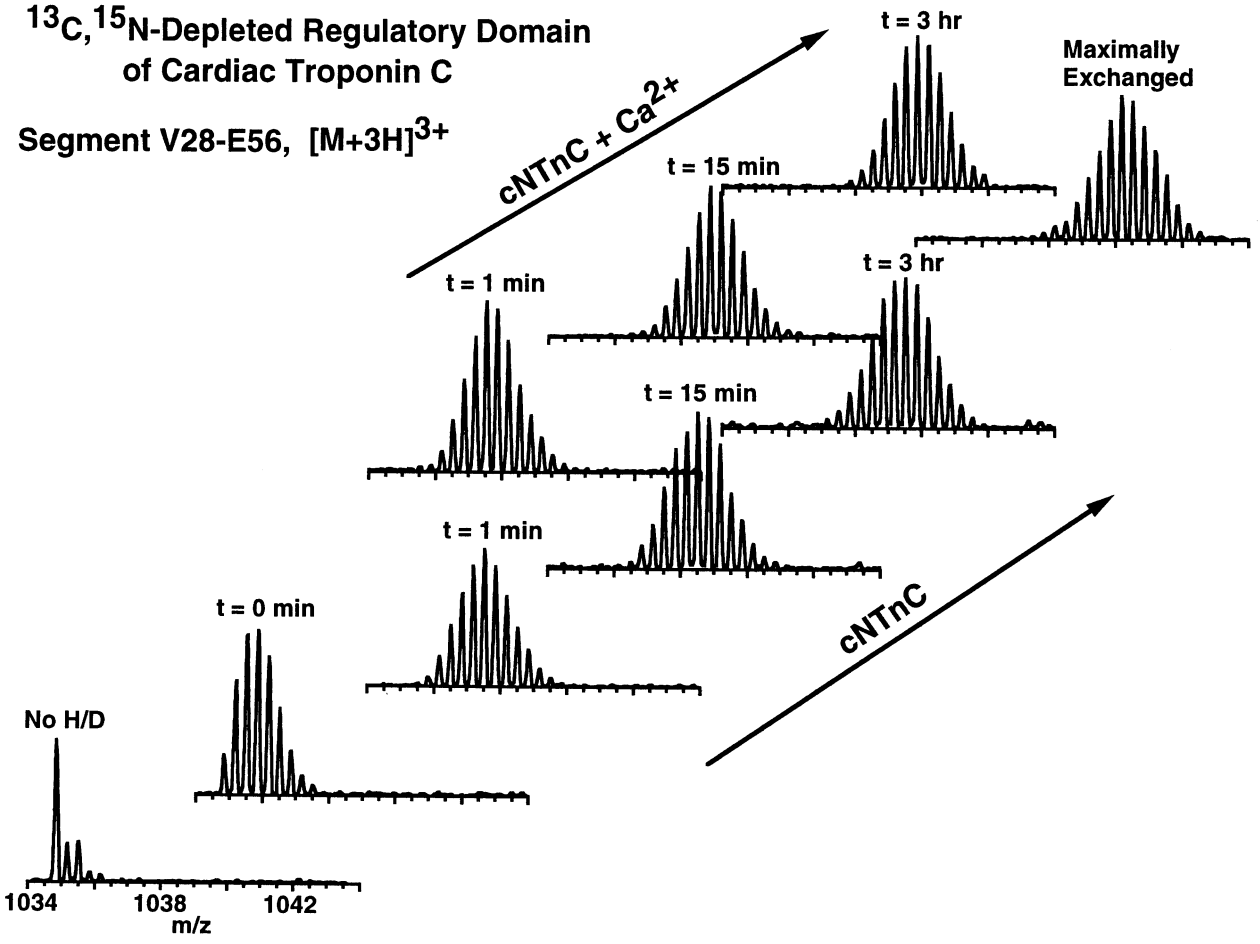

Figure 4. ESI FT-ICR mass spectra of the V28-E56 $[M + 3H]^{3+}$ ion pepsin-cleaved segment from ^{13}C, ^{15}N-depleted cNTnC, following each of various periods of solution-phase H/D exchange. Lower: apo-cNTnC. Upper: Ca^{2+}-saturated cNTnC. Note the small (but detectable) increase in deuterium uptake on binding of Ca^{2+}.

identified in this way! For the remaining 2, more than one peptide sequence matched the experimental mass to within 100 ppm, but the correct peptide could be assigned, based on the previously identified cleavage sites. In all, we identified 12 segments, spanning 100% of the cNTnC primary amino acid sequence (see Figure 1).

Deuterium Incorporation for Various Proteolytic Segments

We measured the time course for deuterium incorporation for each of the 12 available proteolytic peptide segments derived from cNTnC. Figure 2 shows that the proteolytic segments spanning residues 1–11, 8–24, and 25–29 show no significant difference in extent of deuterium incorporation between apo- and Ca^{2+}-saturated forms of cNTnC. However, nine other segments (four of which, spanning residues 28–56, 36–56, 36–64, and 60–89, are shown in Figure 3) exhibited a pronounced increase in extent of deuterium incorporation for Ca^{2+}-complexed cNTnC relative to cNTnC. For example, the number of deuteriums incorporated into segment V28-E56 increases by 3 (i.e., ~10% of a segment consisting of 27 amino acids) on Ca^{2+} binding, after correction for back exchange during the quenching, pepsin digestion, and LC-MS analysis steps. Although small, the difference of 3 Da is much larger than experimental error (see Figure 4), because our LC-ESI FT-ICR MS measurements from three independent runs (including errors introduced from H/D exchange, quenching, pepsin digestion, HPLC, and FT-ICR MS), are reproducible to within 0.5 Da [18]. As a further test, we repeated the H/D exchange of cNTnC for 2 h, both in the apo- and Ca^{2+}-saturated forms of cNTnC, and again observed a statistically significant increase in deuterium incorporation into the same four segments for Ca^{2+}-complexed cNTnC relative to cNTnC.

We have previously pointed out that H/D exchange is best quantitated by its *rate*, rather than by the *extent* of exchange after a particular H/D exchange period [21]. We therefore subjected each deuterium uptake versus

time profile to maximum entropy method (MEM) analysis to determine the most probable rate constant distribution for the (known) number of exchangeable protons in each segment [18, 21]. MEM H/D exchange rate constant distributions corresponding to the deuterium uptake curves in Figure 4 are shown in Figure 5. For well-resolved peaks, the (linear) ordinate in Figure 5 is scaled so that the total area under each peak corresponds to the total number of amide hydrogens (listed above each peak) over the range of exchange rate constants spanning that peak [21]. However, for rate constants too slow (or too fast) to be determined from the experimental data, the MEM rate constant distribution levels off to a horizontal line extending infinitely to the left (or right) in Figure 5.

Interpretation of MEM rate constant distributions is simple. For example, for segment V28-E56 (Figure 5, upper left), two slowly exchanging amide hydrogens ($k \leq 10^{-2}\ h^{-1}$) for apo-cNTnC speed up to an intermediate exchange rate ($10^{-1}\ h^{-1} \leq k \leq 10^{2}\ h^{-1}$) on binding of Ca^{2+}. Finally, for reference, each panel in Figure 5 also lists the total number of potentially exchangeable amide hydrogens for a given segment.

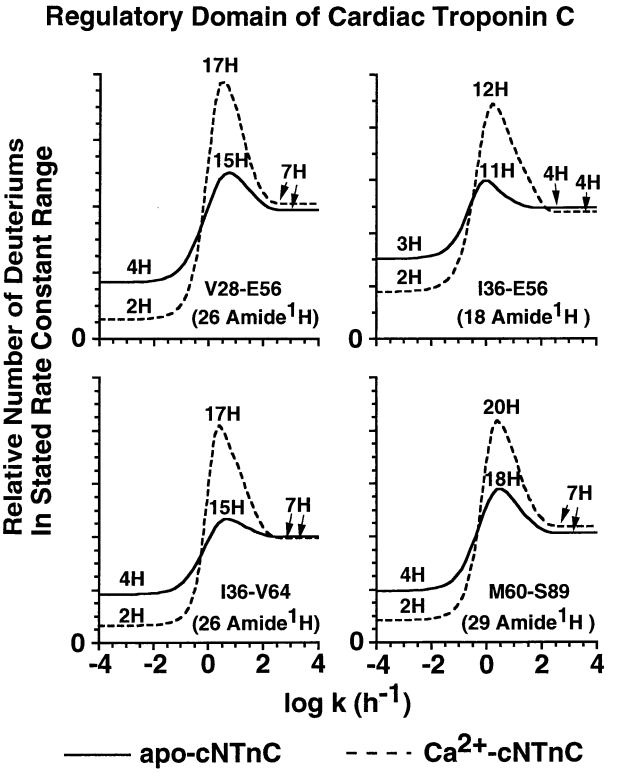

Figure 5. H/D exchange rate constant distributions derived from the H/D exchange time course for each of the four different segments shown in Figure 4: apo-cNTnC (———) and Ca^{2+}-saturated cNTnC (– – – –). The total number of backbone amide hydrogens for each segment is indicated in each panel. The number of backbone amide hydrogens for each resolved peak in the MEM-derived rate constant distribution is shown above that peak.

Visualization of Effects of Calcium Binding on cNTnC Solvent Accessibility

Although it is possible to infer conformational changes on binding of Ca^{2+} within individual segments of cNTnC from the observed differences in exchange rate constant distributions (Figure 5), we find it easier to consider the results graphically by shading the segments of a three-dimensional NMR ribbon structure of cNTnC (Figure 6). In this case, segments exhibiting *increased* H/D exchange on Ca^{2+} binding are shaded darker. In Figure 6, residues 1–11 include helix N (5–11); residues 8–24 include most of helix A (14–26); residues 36–56 include helix B (38–48) and the turn between the B and C helices; residues 28–56 include the turn between the A and B helices comprising calcium binding site I (28–40), helix B (38–48) and the turn between the B and C helices; residues 36–64 include helix B (38–48), the turn between the B and C helices, and helix C (54–64); and residues 60–89 include helix C (54–64), the turn between the C and D helices comprising calcium binding site II (65–76), and helix D (74–84).

Small Conformational Changes Measured by H/D Exchange and LC-ESI FT-ICR MS

Small conformational changes previously detected by H/D exchange and LC-ESI-MS include a minor conformational difference between oxidized and reduced cytochrome *c* [48] and a small change resulting from point mutations of a bacterial phosphocarrier protein [16]; the Gibbs free energy (ΔG) of folding for two mutants is greater than that for the wild type by 1.5 and 0.5 kcal/mol, based on urea denaturation. ΔG of folding for cardiac TnC is not known. However, ΔG of unfolding for Ca^{2+}-saturated skeletal NTnC is greater than that for apo-NTnC by 1.3 kcal/mol [49] based on thermal denaturation. NMR reveals a large-scale movement of helices B and C of sNTnC away from helices N, A, and D after Ca^{2+} binding [50], whereas cNTnC exhibits only minor reorientation of the B and C helices relative to the N/A/D unit on Ca^{2+} binding [45].

The opening of the structure and the exposure of hydrophobic patch are evidently energetically unfavorable for cNTnC [51]. Specifically, the total exposed hydrophobic surface area increases dramatically (by 520 Å^2) from 2866 Å^2 for apo-sNTnC to 3386 Å^2 for Ca^{2+}-sNTnC, but increases almost undetectably (by 18 Å^2, from 3090 ± 86 to 3108 ± 71 Å^2) for the corresponding cardiac isoform [45]. Remarkably, we are easily able to detect this small conformational change of cNTnC upon calcium binding by H/D exchange coupled with pepsin digestion and LC-ESI FT-ICR MS, because we can determine the number of incorporated deuteriums to within 0.5 Da, or to within at most ~3% in that segment by FT-ICR MS [18], compared to within ~5% in prior reports [12, 15].

In summary, solution-phase H/D exchange coupled with proteolytic digestion, high-performance liquid chromatography and ESI FT-ICR MS provides a sensi-

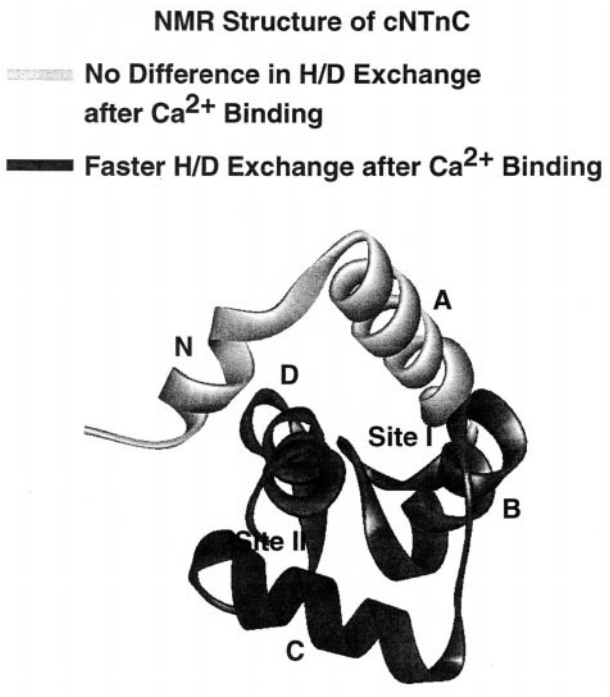

Figure 6. Ribbon diagrams of the three-dimensional NMR structure of calcium saturated cardiac regulatory domain of TnC, drawn with WebLab Viewer. Shading denotes faster (dark), or unchanged (light) deuterium uptake for calcium-saturated cNTnC relative to calcium-free cNTnC.

tive method for the measurement of small ligand-induced conformational or dynamic changes in a protein. Here, we have detected the small reorientation of the B and C helices relative to the N, A, and D helices of the N-terminal domain of human cardiac troponin C upon Ca^{2+} binding. Although more detailed structural details can in principle be obtained by NMR or X-ray crystallography, the mass spectrometry-based approach consumes vastly less sample and requires much less time for analysis. For example, NMR requires ~3 mM × 0.5 ml = 1.5 μmol, or ~15 mg for a 10K protein; where as mass spectrometry requires 10 kinetic runs, each ~25 μM × 15 μL = 10 × 375 pmol, or ~40 μg for a 10K protein. Moreover, mass spectrometry is available for proteins too large (or aggregated or insoluble) for NMR analysis.

Acknowledgments

This work was supported by grants (to AGM) from NSF (CHE-94-13008), NIH (GMj31683), Florida State University, and the National High Magnetic Field Laboratory in Tallahassee, FL, and (to B.D.S.) from the MRC Group in Protein Structure and Function supported by the Medical Research Council of Canada.

References

1. Englander, J. J.; Roger, J. R.; Englander, S. W. Measurement and calibration of peptide group hydrogen-deuterium exchange by ultraviolet spectrophotometry. *Anal. Biochem.* **1979,** *92*, 517–524.
2. Woodward, C.; Simon, I.; Tuchsen, E. Hydrogen exchange and the dynamic structure of proteins. *Mol. Cell. Biochem.* **1982,** *48*, 135–160.
3. Englander, S. W.; Kallenbach, N. R. Hydrogen exchange and structural dynamics of proteins and nucleic acids. *Quart. Rev. Biophys.* **1984,** *16*, 521–655.
4. Gregory, R. B.; Rosenberg, A. Protein conformational dynamics measured by hydrogen isotopic exchange techniques. In *Methods in Enzymology*; Hirs, C. H. W., and Timasheff, S. N., Eds.; Academic: Orlando, 1986; Vol 131, pp 448–508.
5. Englander, S. W.; Mayne, L. Protein folding studied using hydrogen-exchange labeling and two-dimensional NMR. *Annu. Rev. Biophys. Biomol. Struct.* **1992,** *21*, 243–265.
6. Katta, V.; Chait, B. T. Hydrogen/deuterium exchange electrospray ionization mass spectrometry: a method for probing protein conformational changes in solution. *J. Am. Chem. Soc.* **1993,** *115*, 6317–6321.
7. Miranker, A.; Robinson, C. V.; Radford, S. E.; Aplin, R. T.; Dobson, C. M. Detection of Transient Protein Folding Populations by Mass Spectrometry. *Science* **1993,** *262*, 896–900.
8. Wagner, D. S.; Anderegg, R. J. Conformation of cytochrome c studied by deuterium exchange-electrospray ionization mass spectrometry. *Anal. Chem.* **1994,** *66*, 706–711.
9. Wang, F.; Blanchard, J. S.; Tang, X-J. Amide hydrogen exchange/electrospray ionization mass spectrometry studies of substrate and inhibitor binding and conformational changes of *E. coli* dihydrodipicolinate reductase. *Biochemistry* **1997,** *36*, 3755–3759.
10. Chung, E. W.; Nettleton, E. J.; Morgan, C. J.; Grob, M.; Miranker, A.; Radford, S. E.; Dobson, C. M.; Robinson, C. V. Hydrogen exchange properties of proteins in native and denatured states monitored by mass spectrometry and NMR. *Prot. Sci.* **1997,** *6*, 1316–1324.
11. Robison, C. V.; Gross, M.; Eyles, S. J.; Ewbank, J. J.; Mayhew, M.; U., H. F.; Dobson, C. M.; Radford, S. E. Conformation of GroEL-bound α-lactalbumin probed by mass spectrometry. *Nature* **1994,** *372*, 646–651.
12. Zhang, Z.; Smith, D. L. Determination of amide hydrogen exchange by mass spectrometry: A new tool for protein structure elucidation. *Prot. Sci.* **1993,** *2*, 522–531.
13. Smith, D. L.; Zhang, Z. Probing noncovalent structural features of proteins by mass spectrometry. *Mass Spectrom. Rev.* **1994,** *13*, 411–429.
14. Zhang, Z.; Post, C. B.; Smith, D. L. Amide hydrogen exchange determined by mass spectrometry: application to rabbit muscle aldolase. *Biochemistry* **1996,** *35*, 779–791.
15. Johnson, R. S. Mass spectrometric measurement of changes in protein hydrogen exchange rates that result from point mutations. *J. Am. Soc. Mass Spectrom.* **1996,** *7*, 515–521.
16. Remigy, H.; Jaquinod, M.; Y., P.; Gagnon, J.; Cheng, H.; Xia, B.; Markley, J. H.; Hurley, J. K.; Tollin, G.; Forest, E. Probing the influence of mutations on the stability of a ferredoxin by mass spectrometry. *J. Prot. Chem.* **1997,** *16*, 527–532.
17. Resing, K. A.; Ahn, N. G. Deuterium exchange mass spectrometry as a probe of protein kinase activation. Analysis of wild type and constitutively active mutants of MAP kinase Kinase-1. *Biochemistry* **1998,** *37*, 463–475.
18. Wang, F.; Li, W.; Emmett, M. R.; Hendrickson, C. L.; Marshall, A. G.; Zhang, Y.-L.; Wu, L.; Zhang, Z.-Y. Conformational and dynamic changes of Yersinia protein tyrosine phosphatase induced by ligand binding and active site mutation and revealed by H/D exchange and electrospray ionization Fourier transform ion cyclotron resonance mass spectrometry. *Biochemistry* **1998,** *37*, 15289–15299.
19. Johnson, R. S.; Walsh, K. A. Mass spectrometric measurement of protein amide hydrogen exchange rates of apo- and holomyoglobin. *Prot. Sci.* **1994,** *3*, 2411–2418.

20. Zhang, Z.; Li, W.; Li, M.; Logan, T. M.; Guan, S.; Marshall, A. G. Higher-order structure and dynamics of FK506-binding protein probed by backbone amide hydrogen/deuterium exchange and electrospray ionization Fourier transform ion cyclotron resonance mass spectrometry. *Tech. Prot. Chem.* **1997,** *VIII*, 703–713.
21. Zhang, Z.; Li, W.; Logan, T. M.; Li, M.; Marshall, A. G. Human recombinant [C22A] FK506-binding protein amide hydrogen exchange rates from mass spectrometry match and extend those from NMR. *Prot. Sci.* **1997,** *6*, 2203–2217.
22. Wang, F.; Scapin, G.; Blanchard, J. S.; Angeletti, R. H. Substrate binding and conformational changes of *Clostridium glutamicum* diaminopimelate dehydrogenase revealed by H/D exchange and electrospray mass spectrometry. *Prot. Sci.* **1998,** *7*, 293–299.
23. McLafferty, F. W. High-resolution tandem FT mass spectrometry above 10 kDa. *Acc. Chem. Res.* **1994,** *27*, 379–386.
24. Wu, Q.; Van Orden, S.; Cheng, X.; Bakhtiar, R.; Smith, R. D. Characterization of cytochrome c variants with high-resolution FTICR mass spectrometry: Correlation of fragmentation and structure. *Anal. Chem.* **1995,** *67*, 2498–2509.
25. Senko, M. W.; Hendrickson, C. L.; Pasa-Tolic, L.; Marto, J. A.; White, F. M.; Guan, S.; Marshall, A. G. Electrospray ionization FT-ICR mass spectrometry at 9.4 Tesla. *Rapid Commun. Mass Spectrom.* **1996,** *10*, 1824–1828.
26. Kelleher, N. L.; Senko, M. W.; Siegel, M. M.; McLafferty, F. W. Unit resolution mass spectra of 112 kDa molecules with 3 Da accuracy. *J. Am. Soc. Mass Spectrom.* **1997,** *8*, 380–383.
27. Buchanan, M. V.; Hettich, R. L. Characterization of large biomolecules by Fourier transform mass spectrometry. *Anal. Chem.* **1993,** *65*, 245A–259A.
28. Amster, I. J. A tutorial on Fourier transform mass spectrometry. *J. Mass Spectrom.* **1996,** *31*, 1325–1337.
29. Dienes, T.; Pastor, S. J.; Schürch, S.; Scott, J. R.; Yao, J.; Cui, S.; Wilkins, C. L. Fourier transform mass spectrometry—Advancing years (1992-Mid 1996). *Mass Spectrom. Rev.* **1996,** *15*, 163–211.
30. Laude, D. A.; Stevenson, E.; Robinson, J. M. Electrospray ionization/Fourier transform ion cyclotron resonance mass spectrometry. In *Electrospray Ionization Mass Spectrometry*; Cole, R. B., Ed.; Wiley: New York, 1997; pp 291–319.
31. Green, M. K.; Lebrilla, C. B. Ion-molecule reactions as probes of gas phase structures of peptides and proteins. *Mass Spectrom. Rev.* **1997,** *16*, 53–71.
32. Marshall, A. G.; Hendrickson, C. L.; Jackson, G. S. Fourier transform ion cyclotron resonance mass spectrometry: A primer. *Mass Spectrom. Rev.* **1998,** *17*, 1–35.
33. Marshall, A. G.; Senko, M. W.; Li, M.; Dillon, S.; Guan, S.; Logan, T. M. Protein molecular weight to 1 Da by ^{13}C, ^{15}N double-depletion and FT-ICR mass spectrometry. *J. Am. Chem. Soc.* **1997,** *119*, 433–434.
34. Farah, C. S.; Reinach, F. C. The troponin complex and regulation of muscle contraction. *FASEB J.* **1995,** *9*, 755–767.
35. Herzberg, O.; James, M. N. Refined crystal structure of troponin C from turkey skeletal muscle at 2.0 A resolution. *J. Molec. Biol.* **1988,** *203*, 761–79.
36. Potter, J. D.; Gergely, J. The calcium and magnesium binding sites on troponin and their role in the regulation of myofibrillar adenosine triphosphatase. *J. Biol. Chem.* **1975,** *250*, 4628–4633.
37. Putkey, J. A.; Sweeney, H. L.; Campbell, S. T. Site-directed mutation of the trigger calcium-binding sites in cardiac troponin C. *J. Biol. Chem.* **1989,** *264*, 12370–12378.
38. Putkey, J. A.; Liu, W.; Sweeney, H. L. Function of the N-terminal calcium-binding sites in cardiac/slow troponin C assessed in fast skeletal muscle fibers. *J. Biol. Chem.* **1991,** *266*, 14881–14884.
39. Szczesna, D.; Guzman, G.; Miller, T.; Zhao, J.; Farokhi, K.; Ellemberger, H.; Potter, J. D. The role of the four Ca^{2+} binding sites of troponin C in the regulation of skeletal muscle contraction. *J. Biol. Chem.* **1996,** *271*, 8381–8386.
40. Negele, J. C.; Dotson, D. G.; Liu, W.; Sweeney, H. L.; Putkey, J. A. Mutation of the high affinity calcium binding sites in cardiac troponin C. *J. Biol. Chem.* **1992,** *267*, 825–831.
41. Li, M. X.; Gagne, S. M.; Spyracopoulos, L.; Kloks, C. P.; Audette, G.; Chandra, M.; Solaro, R. J.; Smillie, L. B.; Sykes, B. D. NMR studies of Ca^{2+} binding to the regulatory domains of cardiac and E41A skeletal muscle troponin C reveal the importance of site I to energetics of the induced structural changes. *Biochemistry* **1997,** *36*, 12519–12525.
42. Li, M. X.; Chandra, M.; Pearlstone, J. R.; Racher, K. I.; Trigo-Gonzalez, G.; Borgford, T.; Kay, C. M.; Smillie, L. B. Properties of isolated recombinant N and C domains of chicken troponin C. *Biochemistry* **1994,** *33*, 917–1925.
43. Li, M. X.; Gagne, S. M.; Tsuda, S.; Kay, C. M.; Smillie, L. B.; Sykes, B. D. Calcium binding to the regulatory N-domain of skeletal muscle troponin C occurs in a stepwise manner. *Biochemistry* **1995,** *34*, 8330–8340.
44. Gagne, S. M.; Tsuda, S.; Li, M. X.; Smillie, B. D.; Sykes, B. D. Structures of the troponin C regulatory domains in the apo and calcium-saturated states. *Nat. Struct. Biol.* **1995,** *2*, 784.
45. Spyracopoulos, L.; Li, M. X.; Sia, S. K.; Gagne, S. M.; Chandra, M.; Solaro, R. J.; Sykes, B. D. Calcium-induced structural transition in the regulatory domain of human cardiac troponin C. *Biochemistry* **1997,** *36*, 12138–12146.
46. Sia, S. K.; Li, M. X.; Spyracopoulos, L.; Gagne, S. M.; Liu, W.; Putkey, J. A.; Sykes, B. D. Structure of cardiac muscle troponin C unexpectedly reveals a closed regulatory domain. *J. Biol. Chem.* **1997,** *272*, 18216–18221.
47. Senko, M. W.; Hendrickson, C. L.; Emmett, M. R.; Shi, S. D.-H.; Marshall, A. G. External accumulation of ions for enhanced electrospray ionization Fourier transform ion cyclotron resonance mass spectrometry. *J. Am. Soc. Mass Spectrom.* **1997,** *8*, 970–976.
48. Dharmasiri, K.; Smith, D. L. Regional stability changes in oxidized and reduced cytochrome c located by hydrogen exchange and mass spectrometry *J. Am. Soc. Mass Spectrom.* **1997,** *8*, 1039–1045.
49. Fredricksen, R. S.; Swenson, C. A. Relationship between stability and function for isolated domains of troponin C. *Biochemistry* **1996,** *35*, 14012–14026.
50. Slupsky, C. M.; Sykes, B. D. NMR solution structure of calcium-saturated skeletal muscle troponin C. *Biochemistry* **1995,** *34*, 15953–15964.
51. Foguel, D.; Suarez, M. C.; Barbosa, C.; Rodrigues, Jr., J. J.; Sorenson, M. M.; Smillie, L. B.; Silva, J. L. Mimicry of the calcium-induced conformational state of troponin C by low temperature under pressure. *Proc. Natl. Acad. Sci. USA* **1996,** *93*, 10642–10666.